Development of a single-phase half-bridge active power filter with the function of uninterruptible power supplies

W.-L.Lu, S.-N.Yeh, J.-C.Hwang and H.-P.Hsieh

Abstract: Analysis and implementation of a single-phase half-bridge active power filter with the function of uninterruptible power supplies is presented. The system provides the combined functions of battery bank energy storage, power-factor compensation, harmonics elimination and uninterruption of the power supply. When the utility is in normal operation, the proposed system will not only supply DC power for battery charging, but also function as an active power filter for improving the power factor and reducing the current harmonics on the utility side. If the utility power fails, the proposed system will function as an inverter immediately, to supply the battery power to the AC load. Analysis for the proposed system is given first, and a personal computer is then used to implement digitised control of the proposed system to facilitate experimental evaluations for a 1kVA prototype. The feasibility and multi-functional results obtained indicate that the proposed system can be realised by using a digital signal processor as the core controller for cost reduction and reliability enhancement.

List of symbols

d_1, d_2 = switching functions of the insulated-gate bipolar transistors (IGBTs)
d_1^* = duty ratio of d_1
i_a = current of the AC-side inductor, L_a
i_a^* = command current of i_a
i_{bl} = current of the battery-side inductor, L_{bl}
i_{bl}^* = command current of i_{bl}
I_{bl}^* = average command current of ibl^*
i_{cs} = current of AC-side filter capacitor, C_s
i_{cs}^* = command current of i_{cs}
I_1 = fundamental component of the load current
i_L = load current
i_{Ld} = absolute value of i_L
I_n = amplitude of the nth-order harmonic of the load current
i_s = source current
i_s^* = command of source current, i_s
I_{sm}^* = amplitude of source command current
I_{sm1} = amplitude of real component of the fundamental load current
I_{sm2} = the part of the amplitude of the source command contributed to by the battery-charging power
i_u = unit sine wave in phase with v_s
$K_{P1} \sim K_{P4}$ = proportional controllers gain
$K_{I1} \sim K_{I4}$ = integral controllers gain
P_L = average real power of load in one utility cycle
T = period of source
T_{sw} = switching period of the IGBT
V_{cb} = average voltage of v_{cb} in one utility cycle
V_m = peak value of the source voltage
v_b = voltage of battery bank
v_{blmt} = battery-gassing voltage
v_{ca} = $v_{ca1} + v_{ca2}$, voltage of the DC-link capacitor, C_a
v_{ca}^* = command voltage of v_{ca}
$\bar{v}_{ca}$ = average voltage of v_{ca}
Δv_{ca} = $v_{ca}^* - \bar{v}_{ca}$
v_{cb} = voltage of the battery filter capacitor, C_b
v_{cb}^* = command voltage of v_{cb}
Δv_{cb} = $v_{cb}^* - v_{cb}$
v_{co} = voltage of the load-side DC filter capacitor, C_o
v_{cs} = v_L, voltage of the AC filter capacitor, C_s
v_{drop} = diode forward voltage
v_L^* = command voltage of v_L
Δv_L = $v_L^* - v_L$
v_s = source voltage
θ_n = phase of the nth-order harmonic of the load current
ω = angular frequency of source

1 Introduction

Since power-electronics techniques are widely applied to industrial devices, a great number of single-phase nonlinear loads, such as AC/DC motor drives, AC/DC power supplies and lighting loads etc., usually introduce harmonics

IEE Proceedings online no. 20000438
DOI: 10.1049/ip-epa:20000438
Paper received 27th January 2000

The authors are with the Department of Electrical Engineering, National Taiwan University of Science and Technology, 43, Section 4, Keelung Road, Taipei, Taiwan 106, Republic of China

into the utility. They also cause poor input power factors and low efficiency, and result in the destruction of other equipment. To improve the power quality of utilities, many single-phase active power filters have been proposed [1–3]. The active power filters inject a compensation current into the utility to maintain the source current as a sine wave in phase with the utility voltage.

Generally, diesel-engine generators are used as the spare power, however, they can not be started immediately. This necessitates the use of an uninterruptible power supply (UPS) [4] to keep the load operating until the utility power is recovered or the spare power takes over. Several researchers [5–7] have focused on a system which combines the functions of an active power filter and a UPS. However, there has been little work published on the increase of the life cycle of the battery with respect to its charging and discharging operations.

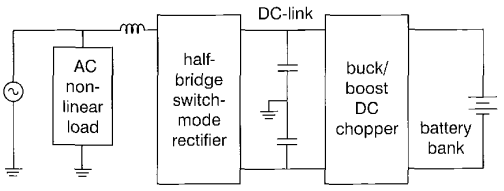

Fig. 1 *Block diagram of the proposed system*

This paper presents the design and implementation of a single-phase half-bridge active power filter with the function of uninterruptible power supplies. It combines the functions of an active power filter, battery-energy storage and a UPS, which together improve the power quality and reliability of the utility. Fig. 1 shows the block diagram of the proposed system. It is seen from Fig. 1 that, on the utility side, a half-bridge switch-mode rectifier [8–10] is used as either an active power filter or inverter. The charging and discharging of the battery bank are conducted by a buck/boost DC chopper [11]. When the utility is normal, the proposed system, which serves as an active power filter, calculates the current command of the rectifier from the load current and the required energy of the battery to control the source power, with improved input harmonics and power factor. Meanwhile, depending on the voltage level of the battery bank, the constant-current and constant-voltage control methods are applied alternately to control the DC chopper, which sustains the battery life. When the utility fails, the half-bridge switch-mode rectifier will function quickly as an inverter to supply the power to the load. The DC chopper discharges the battery to keep the DC-link voltage at a fixed level. To overcome the transient delay due to the mode change, a power balance and feedforward [12] control methods will be applied to improve the performance. In addition, a current-predicted control [13, 14] technique will be used to determine the switching states of the half-bridge switch-mode rectifier. Simulated and experimental results for a 1kVA prototype indicate that the total harmonic distortion of the input current is reduced from 45.9% to 7.3% with a near-unity power factor for the nonlinear load. In addition, the mode change will be finished within 1.5ms, in both the cases of power failure and power recovery, and so the system is operated as an uninterruptible power supply.

2 Power circuit

The power circuit of the proposed system is shown in Fig. 2. It is seen from Fig. 2 that the proposed system contains two insulated-gate bipolar-transistor (IGBT) modules. T_a^+ and T_a^- are the first pair of IGBT modules which is used in the half-bridge switch-mode rectifier for AC/DC conversion, while T_b^+ and T_b^- are the second pair of IGBT modules which is used in the buck/boost DC chopper for DC/DC conversion. The DC-link is a cascaded connection using two identical capacitors C_{a1} and C_{a2}. L_a, C_s, L_{bl} and C_b are used for attenuating high-frequency components. FS_{w1} and FS_{w2} are fast AC switches. When the utility is in normal operation, FS_{w1} is turned on and FS_{w2} is turned off, the system functions as an active power filter and the battery bank is in the energy-storage mode. On the other hand, when the utility fails, FS_{w2} is turned on and FS_{w1} is turned off, and the system is in inverter mode, functioning as an uninterruptible power supply.

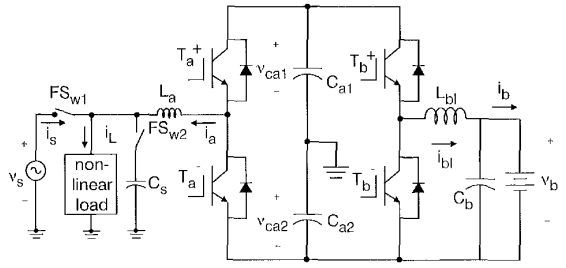

Fig. 2 *Power circuit of the proposed system*

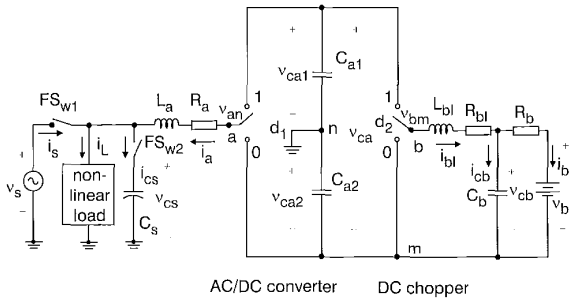

Fig. 3 *The equivalent circuit for the proposed system*

It is noted in Fig. 2 that the two IGBTs which belong to the same module cannot be turned on simultaneously. For example, when T_a^+ is on, T_a^- is off, and vice versa. Assume that the IGBTs are ideal switches with the switching functions d_1 and d_2. When T_a^+ is on, $d_1 = 1$, whereas when T_b^+ is on, $d_2 = 1$. Thus Fig. 2 can be simplified to its equivalent circuit shown in Fig. 3.

From the above discussion, it is obvious from Figs. 2 and 3 that only one of the two switching devices of each IGBT module can conduct at any one instant. This indicates that the proposed system can be expected to operate highly efficiently [9].

From Fig. 3, one obtains the state equation of the proposed system as follows:

$$L_a \frac{d}{dt} i_a = -\nu_s - R_a i_a + d_1 \nu_{ca1} - (1 - d_1)\nu_{ca2} \quad (1)$$

$$L_{bl} \frac{d}{dt} i_{bl} = d_2 \nu_{ca1} + d_2 \nu_{ca2} - R_{bl} i_{bl} - \nu_{cb} \quad (2)$$

$$C_{a1} \frac{d}{dt} \nu_{ca1} = -d_1 i_a - d_2 i_{bl} \quad (3)$$

$$C_{a2} \frac{d}{dt} \nu_{ca2} = (1 - d_1) i_a - d_2 i_{bl} \quad (4)$$

$$C_s \frac{d}{dt} \nu_{cs} = i_s + i_a - i_L \quad (5)$$

$$C_b \frac{d}{dt} v_{cb} = i_{bl} - (v_{cb} - v_b)/R_b \quad (6)$$

It is seen from eqns. 1–6 that if the DC-link command voltage is v_{ca}^* and the command current of the battery-side inductor is i_{bl}^*, one can feed back the voltages v_s, v_{ca}, v_{cb}, v_{cs} and the currents i_a, i_L, i_{bl} to design the switching functions d_1 and d_2 for the proposed system.

To better illustrate the effect of the system in both the rectifier and inverter modes, a typical nonlinear load, such as the single-phase full-bridge rectifier shown in Fig. 4, is introduced deliberately. Besides diodes, other elements of Fig. 4 include a smoothing capacitor C_o, a series inductor L_s and a resistance R_o which characterises the DC load.

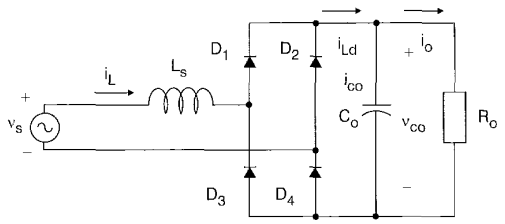

Fig. 4 *A single-phase nonlinear load circuit*

From Fig. 4, the state equations of the nonlinear load on the DC side can be expressed as follows [15]:

$$L_s \frac{d}{dt} i_{Ld} = |v_s| - v_{co} - 2v_{drop} \quad \text{if } |v_s| > v_{co}$$
$$= 0 \quad \text{otherwise} \quad (7)$$

$$C_o \frac{d}{dt} v_{co} = i_{Ld} - v_{co}/R_o \quad (8)$$

Based on eqns. 1–8, the decision of the control parameters and the computer simulation for the proposed system will be given.

3 Control of the multi-function system

In this paper, a current-control scheme is used to control the switch-mode rectifier and the buck/boost DC chopper. Before deciding the IGBTs' switching functions, the command currents i_a^* and i_{bl}^* of the inductors must be calculated first. These are derived below.

3.1 Active power filter mode

Let the utility voltage be sinusoidal and represented by

$$v_s = V_m \sin \omega t \quad (9)$$

Also let the nonlinear load current be expressed by

$$i_L = \sum_{n=1}^{\infty} I_n \sin(n\omega t + \theta_n)$$
$$= I_1 \sin(\omega t + \theta_1) + \sum_{n=2}^{\infty} I_n \sin(n\omega t + \theta_n) \quad (10)$$

Assume that i_u is the unit sine wave and in-phase with the source voltage. Using Fourier analysis, one can obtain the amplitude of the real component of the fundamental load current, which is in-phase with the source voltage as

$$I_{sm1} = \frac{2}{T} \int_0^T i_L i_u dt = I_1 \cos\theta_1 \quad (11)$$

Physically, I_{sm1} is the amplitude of the utility current, which provides the average real power for the nonlinear load. In this paper, the I_{sm1} of eqn. 11 was calculated by integrating the term $2i_L i_u$, which was sampled, held and reset by the zero-crossing signal of the utility voltage in every utility cycle. Referring to Fig. 2, it is seen that the utility will supply the real power for not only the nonlinear load but also the battery charging and system operation loss. In the steady state, the real power of the system will balance in one utility cycle. From Fig. 2, it can be found that if the nonlinear load is switched off, the system operation loss is negligible, the source current is a sine wave, which is in phase with the source voltage and with an amplitude of I_{sm2}, and the amplitude of the source current I_{sm2} can be obtained as

$$I_{sm2} = 2V_{cb} I_{bl}^* / V_m \quad (12)$$

In addition, to ensure proper operation for the half-bridge switch-mode rectifier [9], a proportion-integral (PI) controller is used to keep the DC-link voltage above $2V_m$. Thus the amplitude of the source command current can be represented by

$$I_{sm}^* = \left(K_{P1} \Delta v_{ca} + K_{I1} \int \Delta v_{ca} dt \right) + I_{sm1} + I_{sm2} \quad (13)$$

The source command current can then be obtained by multiplying I_{sm}^* by i_u as

$$i_s^* = I_{sm}^* \sin \omega t \quad (14)$$

From Fig. 2, the active power filter compensation current i_a^* can be calculated by subtracting the source command current i_s^* from the load current i_L. This yields

$$i_a^* = i_L - i_s^* \quad (15)$$

The control block diagram of i_a^* is shown in Fig. 5.

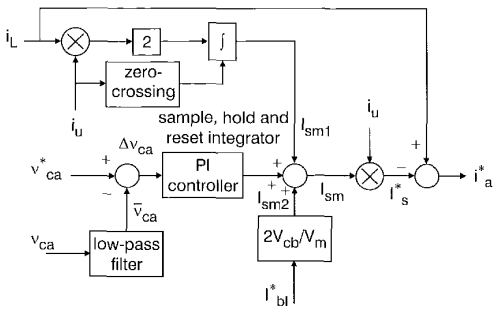

Fig. 5 *Block diagram of the compensation current command, i_a^**

3.2 Inverter mode

When the utility fails, the half-bridge switch-mode rectifier is operated in the inverter mode. Consequently, the DC-link capacitors can supply the power to the nonlinear load uninterruptedly with appropriate control of the duty ratio d_1. To minimise the effect of the load voltage fluctuation, the output command voltage of the inverter will be in phase with the utility as power outage occurs. It can be represented by

$$v_{cs}^* = v_L^* = V_m \sin \omega t \quad (16)$$

From eqn. 16, one can obtain the command current of the filter capacitor C_s as

$$i_{cs}^* = C_s \frac{dv_L^*}{dt} = \omega C_s V_m \cos \omega t \quad (17)$$

The output voltage of the inverter will be affected by a change of load. Assuming that the fluctuating voltage of the load is $\Delta v_L = v_L^* - v_L$, one can obtain appropriate compensation using a proportion-integral controller. To improve the transient response, the load current i_L is also added to command current for feedforward control. This gives the inverter output command current

$$i_a^* = i_{cs}^* + \left(K_{P2}\Delta v_L + K_{I2}\int \Delta v_L dt\right) + i_L \quad (18)$$

In this paper, the current control of the half-bridge switch-mode rectifier is modelled using the current-predicted control technique [13, 14]. The error between the command current and the actual current is used to compute the switching duty ratio in one period. Owing to the fact that the utility frequency is much lower than the switching frequency, the switching function d_1 can be replaced by its duty ratio d_1^* [14], and eqn. 1 can then be rewritten as

$$v_s + R_a i_a + L_a \frac{d}{dt} i_a = d_1^* v_{ca1} - (1 - d_1^*) v_{ca2} \quad (19)$$

Assume that T_{sw} is the switching period. Then

$$\frac{d}{dt} i_a = \frac{1}{T_{sw}}(i_a^* - i_a) \quad (20)$$

Substituting eqn. 20 into eqn. 19, one obtains the duty ratio command of the first IGBT module, d_1^*, as

$$d_1^* = \frac{1}{v_{ca}}\left[v_s + \left(R_a - \frac{L_a}{T_{sw}}\right) i_a + \frac{L_a}{T_{sw}} i_a^* + v_{ca2}\right] \quad (21)$$

It can easily be seen from eqn. 21 that using the duty ratio command d_1^*, the actual current can follow the command current in one period at high switching frequency. The voltage v_{ca2} in eqn. 21 can be replaced by $0.5v_{ca}$ for implementation, and the voltage v_s in eqn. 21 can be replaced by v_{cs} for inverter-mode control.

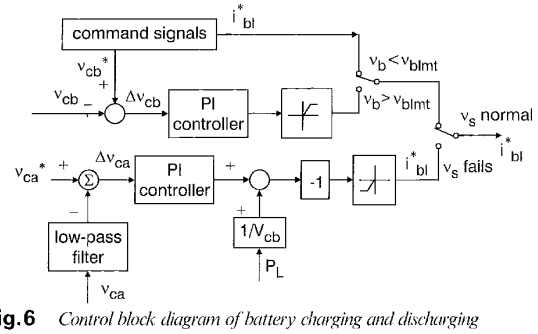

Fig. 6 *Control block diagram of battery charging and discharging*

3.3 Battery charging and discharging

Fig. 6 is the control block diagram of the battery charging and discharging. When the utility is normal, the DC chopper operates in the buck chopper mode to store the energy from the DC-link to the batteries. The optimum charging operation adopted is a two-step constant-current and constant-voltage charging. When the battery voltage is below the gassing voltage, v_{blmt}, constant-current charging is used to reduce the charging time. When the battery voltage approaches the gassing voltage, constant-voltage charging is exercised to maintain the battery capacity. Thus, the constant-voltage charging current command i_{bl}^* can be expressed as

$$i_{bl}^* = K_{P3}\Delta v_{cb} + K_{I3}\int \Delta v_{cb} dt \quad (22)$$

When the utility fails, the DC chopper operates at boost chopper mode and the battery discharges quickly to keep the DC-link voltage at the voltage command v_{ca}^*. In the steady state, if the system operation loss is negligible, the battery discharging power will be equal to the real power of the nonlinear load in one utility cycle. Then, the battery discharging command current can be written as

$$i_{bl}^* = -\left(\left(K_{P4}\Delta v_{ca} + K_{I4}\int \Delta v_{ca} dt\right) + P_L / V_{cb}\right) \quad (23)$$

In eqn. 23, P_L is the average real power of the load in each cycle. It can be calculated from I_{sm1} of eqn. 11 as

$$P_L = (V_m I_{sm1})/2 \quad (24)$$

The feedforward control can be accomplished by the last term on the right-hand side of eqn. 23 to improve the transient response. The current control of the DC chopper is modelled using the hysteresis current-control method, to avoid the change of parameters due to battery charging and discharging.

4 Simulation and experimental results

To verify the performance of the proposed system, the complete system was simulated using the MATLAB-SIMULINK software package and a 1kVA prototype was built and tested. The control block diagram of the proposed system is shown in Fig. 7. The major parameters used in the simulation and implementation of Fig. 7 are as follows: AC source voltage = 110Vrms (60Hz), DC-link capacitors $C_{d1} = C_{d2} = 3000\mu F$, AC capacitor $C_s = 40\mu F$, inductor $L_a = 3.6mH$, inductor $L_{bl} = 9.6mH$, battery bank voltage = 175V, (14 pieces, 12V, 24Ah batteries serial), inductor $L_s = 4mH$, load capacitor $C_o = 3000\mu F$, load resistance $R_o = 17.5\Omega$, digital controller switching period $T_s = 100\mu s$, and the control parameters are $K_{P1} = 1.3$, $K_{I1} = 16$, $K_{P2} = 1.8$, $K_{I2} = 36$, $K_{P3} = 1.2$, $K_{I3} = 10$, $K_{P4} = 0.1$, $K_{I4} = 1.2$.

The experimental results of the nonlinear load are shown in Fig. 8, where the load is 1kVA and the utility-side input power factor is 0.78. Fig. 8*c* is the spectrum of the utility current. There exists large harmonics at 180Hz, 300Hz, 420Hz etc., and the total harmonic distortion of the utility current is 45.9%. Figs. 9 and 10 show the simulated and experimental results of normal operation, respectively, where the DC-link voltage command v_{ca}^* is 360V, the load is 1kVA, the battery charging current is 1A and the utility-side total input power is 1.04kVA. Fig. 10*d* is the spectrum of an experimental source current whose total harmonic distortion is improved to 7.3%. In this case, the utility-side input power factor is 0.995 and the system efficiency is 92.4%. When the battery charging is removed, the utility-side total input power is 815VA, the input power factor is 0.993 and the system efficiency has been increased to 96.3%. Figs. 11 and 12 show the simulated and experimental results for the transient response of the utility-break, where the load is 1kVA and the battery charging current is 0.5A. It can be seen from Fig. 12*e* that the battery discharges quickly. In addition, it is obvious from Fig. 12*c* that, even in the case of the utility failure, the inverter supplies the load with only 1.5ms delay and in phase with the utility. When the system is in the inverter mode with full-load operation, the total harmonic distortion of the load voltage is 3.2%. Fig. 13 shows the transient response of the experimental results, before and after utility power recovery, where the corresponding load is 1kVA and the battery charging current is 0.5A. When the utility power

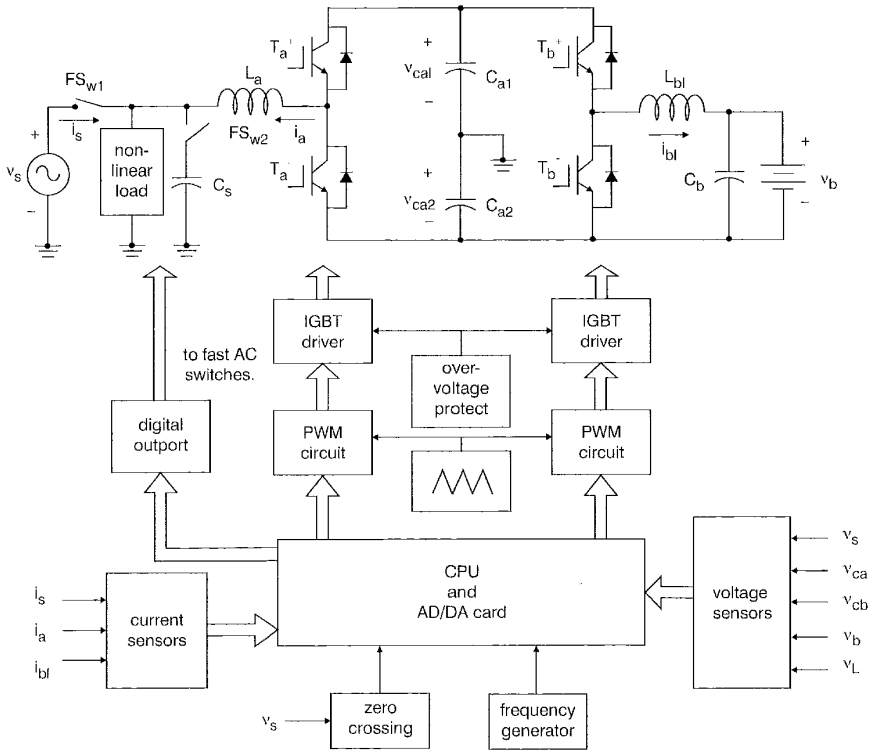

Fig. 7 *The control block diagram of the proposed system*

recovers, the system operates at the inverter mode until the inverter voltage is in phase with the utility voltage. From Fig. 13*c*, it can be seen that the load voltage is almost in phase with the utility voltage when the system changes the operation mode from inverter to active power filter. Finally, it is important to note, from Figs. 9–12, the close agreement between the corresponding simulation and experimental results.

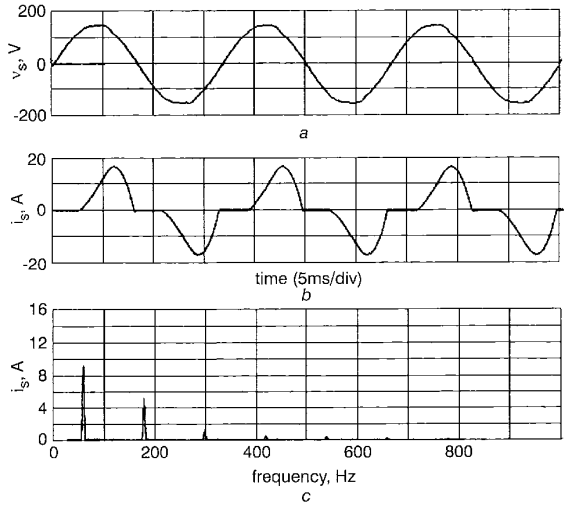

Fig. 8 *The experimental results of a 1kVA nonlinear load*
a Source voltage, v_s
b Source current, i_s
c The spectrum of the source current, i_s

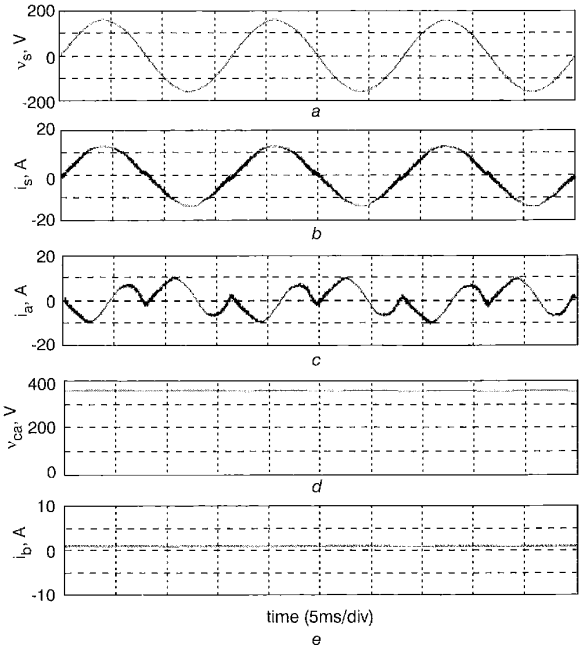

Fig. 9 *Simulated results for the active power filter with a 1kVA load and battery charging current of 1A*
a Source voltage, v_s
b Source current, i_s
c Compensation current, i_a
d DC-link voltage, v_{ca}
e Battery current, i_b

5 Conclusions

In this paper, a single-phase high performance half-bridge active power filter with the function of the uninterruptible power supplies was explored. The operation with the proposed system configuration, which combines the functions of the active power filter, energy storage and uninterruptible power supplies, is verified by simulation and the experimental results of a 1kVA prototype. A personal computer is used to implement digitised control of the system. The results demonstrate that the system possesses a near-unity

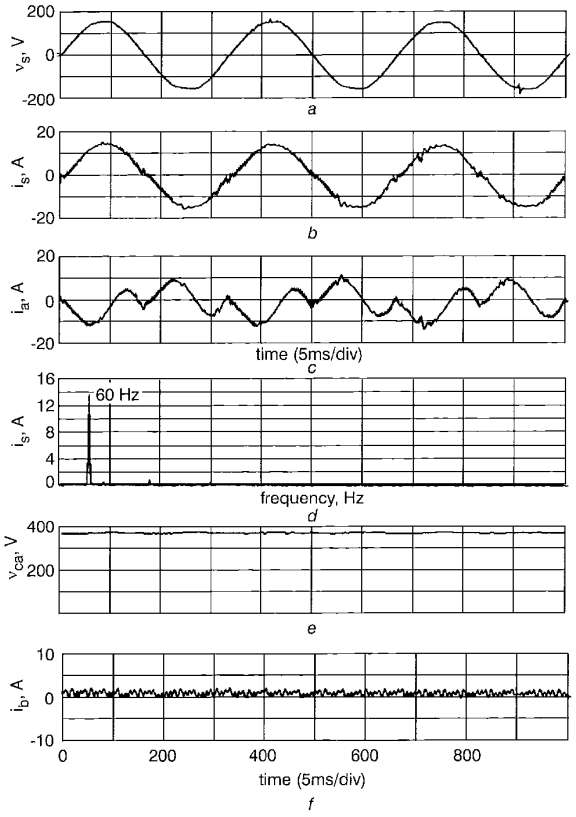

Fig. 10 *Experimental results for the active power filter with a 1kVA load and battery charging current of 1A*
a Source voltage, v_s
b Source current, i_s
c Compensation current, i_a
d The spectrum of the source current, i_s
e DC-link voltage, v_{ca}
f Battery current, i_b

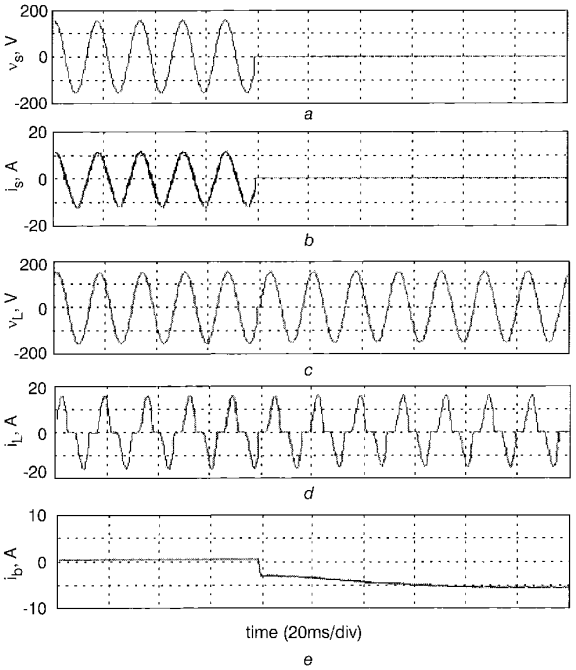

Fig. 11 *UPS simulated results with a 1kVA load and 0.5A charging current breaks*
a Source voltage, v_s
b Source current, i_s
c Load voltage, v_L
d Load current, i_L
e Battery current, i_b

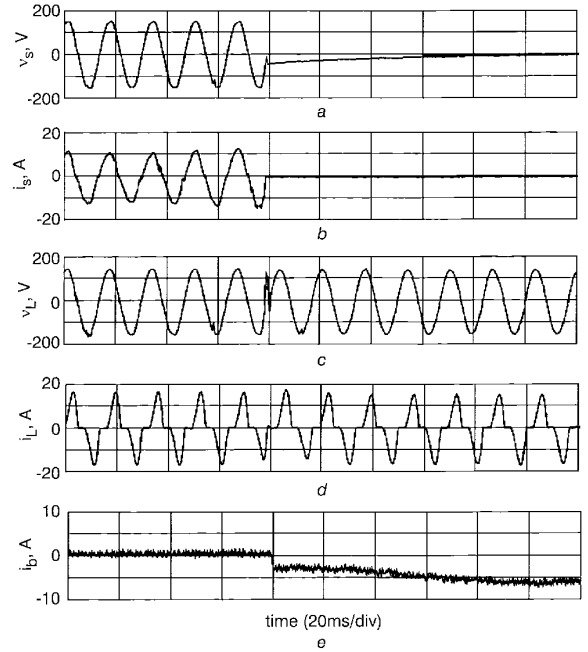

Fig. 12 *UPS experimental results with a 1kVA load and 0.5A charging current breaks*
a Source voltage, v_s
b Source current, i_s
c Load voltage, v_L
d Load current, i_L
e Battery current, i_b

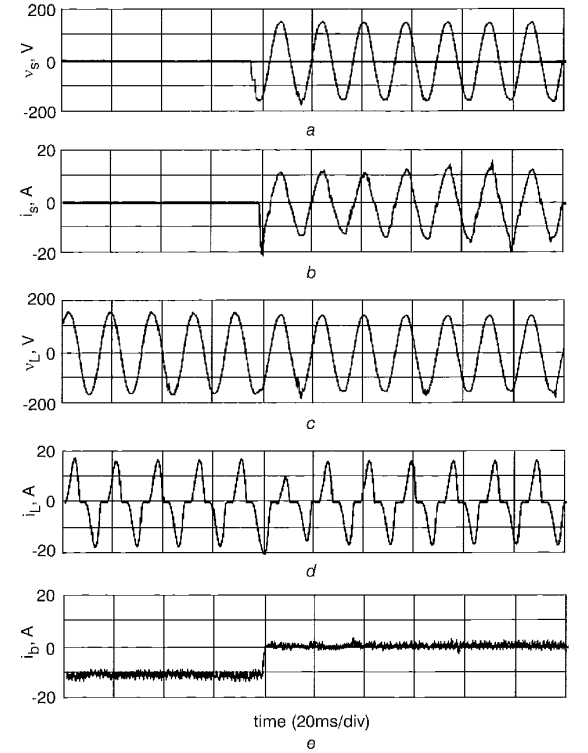

Fig. 13 *UPS experimental results during power recovery with a 1kVA load and battery charging current of 0.5A*
a Source voltage, v_s
b Source current, i_s
c Load voltage, v_L
d Load current, i_L
e Battery current, i_b

power factor and low harmonics on the utility side. In addition, the system efficiency is excellent and the load operates uninterruptedly. The performance evaluation also

indicates that a fast transient response is obtained using a power balance and feedforward control scheme. It is also worth noting that the load voltage is almost in phase with the utility voltage in both the cases of power failure and power recovery. As discussed above, the proposed UPS, when widely used, can effectively improve the quality and reliability of the power utility. In order to reduce the cost, a digital signal processor (DSP) should be used to implement digitised control of the proposed system in the future.

6 Acknowledgment

The authors wish to express their sincere appreciation to the National Science Council for supporting this research with grant NSC 88-2213-E-011-079.

7 References

1 JOU, H.L., WU, J.C., and CHU, H.Y.: 'New single-phase active power filter', *IEE Proc., Electr Power Appl.*, 1994, **141**, (3), pp. 129–134
2 HSU, C.Y., and WU, H.Y.: 'A new single-phase active power filter with reduced energy-storage capacity', *IEE Proc., Electr Power Appl.*, 1996, **143**, (1), pp. 25–30
3 SINGH, B., CHANDRA, A., and AL-HADDAD, K.: 'An improved single phase active power filter with optimum DC capacitor'. Proceedings of IEEE IECON'95, 1996, Vol. 2, pp. 677–682
4 KUBO, I., OZAWA, Y., NAKATSUKA, R., and SHIMIZU, A.: 'A fully digital controlled UPS using IGBT's'. IEEE Conference Record of the 1991 Industry Applications Society Annual Meeting, 1991, Vol. 1, pp. 1042–1046
5 QIN, Y., and DU, S.: 'A DSP based active power filter for line interactive UPS'. Proceedings of IEEE IECON'95, 1995, Vol. 2, pp. 884–888
6 CHOI, J.H., PARK, G.W., and DEWAN, S.B.: 'Standby power supply with active power filter ability using digital controller'. Proceedings of IEEE APEC'95, 1995, Vol. 2, pp. 783–789
7 JOU, H.L., and WU, J.C.: 'A new parallel processing UPS with the performance of harmonic suppression and reactive power compensation'. Proceedings of IEEE PESC'94, 1994, Vol. 2, pp. 1443–1450
8 BOYS, J.T., and GREEN, A.W.: 'Current-forced single-phase reversible rectifier', *IEE Proc., Electr Power Appl.*, 1989, **136**, (5), pp. 205–211
9 SRINIVASAN, R., and ORUGANTI, R.: 'A unity power factor converter using half-bridge boost topology', *IEEE Trans. Power Electron.*, 1998, **13**, (3), pp. 487–500
10 HWANG, J.C., and YEH, S.N.: 'Design and implementation of a single-phase half-bridge switch-mode rectifier', *J. Chin. Inst. Electr. Eng.*, 1998, **5**, (3), pp. 213–221
11 HIMMELSTOSS, F.A.: 'Analysis and comparison of half-bridge bidirectional DC-DC converters'. Proceedings of IEEE PESC'94, 1994, Vol. 2, pp. 922–928
12 OGASAWARA, S., YAMAGISHI, N., TOTSUKA, H., and AKAGI, H.: 'A voltage-source PWM rectifier-inverter with feedforward control of instantaneous power', *Electr. Eng. Jpn.*, 1993, **113**, (4), pp. 113–122
13 KIM, J.M.S., SHANKER, P., and ZHANG, W.: 'Analysis of predictive control for active power factor correction'. Proceedings of IEEE IECON'94, 1994, pp. 446–451
14 WU, R., DEWAN, S.B., and SLEMON, G.R.: 'A PWM AC-to-DC converter with fixed switching frequency', *IEEE Trans. Ind. Appl.*, 1990, **26**, (5), pp. 880–885
15 LAI, J.S.: 'Power electronics system modeling and simulation'. IEEE Conference Record of the 4th Workshop on *Computers in power electronics*, 1994, pp. 45–55